RESEARCH PAPER

Evaluation of 5-aminolevulinic acid-functionalized gold nanoclusters for combined photodynamic and radiation therapy in K562 leukemia cells

Hossein Khosravi[1], Soheila Saeedi[2], Alireza Goodarzi[3], Safoora Nikzad[4], Fatemeh Amiri[3], Abbas Farmani[5]*

[1] Department of Radiology, School of Allied Medical Sciences, Hamadan University of Medical Sciences, Hamadan, Iran
[2] Department of Health Information Technology, School of Allied Medical Sciences, Hamadan University of Medical Sciences, Hamadan, Iran
[3] Department of Medical Laboratory Sciences, School of Paramedicine, Hamadan University of Medical Sciences, Hamadan, Iran
[4] Department of Medical Physics, Faculty of Medicine,Isfahan University of Medical Sciences, Isfahan, Iran
[5] Dental Implant Research Center, Hamadan University of Medical Sciences, Hamadan, Iran

ABSTRACT

Objective(s): The present work investigated the therapeutic potential of 5-aminolevulinic acid-functionalized gold nanoparticles (5-ALA-AuNPs) when combined with radiotherapy (RT) and photodynamic therapy (PDT) in K562 leukemia cells. Particular attention was given to whether altering the order in which RT and PDT were administered could affect the resulting therapeutic response.

Materials and Methods: For the treatment experiments, K562 cells were plated in 96-well culture plates at 10,000 cells per well. The cells were then exposed to 5-ALA-AuNPs at three concentrations (1.25, 0.625, and 0.3125 mg/mL). Treatment groups were subsequently subjected to either laser irradiation (810 nm, 0.1 W for 5 s), X-ray exposure (2 or 4 Gy at 6 MeV), or a combination of the two modalities administered in different sequences. Viability was quantified by the MTT assay 48 h following completion of the treatments.

Results: Among all treatment regimens, the administration of laser irradiation prior to X-ray exposure at 4 Gy in the presence of 5-ALA-AuNPs resulted in the lowest cell survival rate (2.1%). Higher nanoparticle concentrations correlated with greater cytotoxicity. The treatment sequence significantly impacted outcomes, with the "laser-before-radiotherapy" protocol demonstrating superior efficacy.

Conclusions: 5-ALA-AuNPs exhibit potential as dual radiosensitizing and photosensitizing agents. The sequence of irradiation is a critical determinant of therapeutic outcome, with laser priming prior to RT showing the greatest promise. However, due to the absence of detailed physicochemical characterization and mechanistic validation (e.g., ROS, apoptosis, cellular uptake), these findings are preliminary. Further studies are essential to confirm clinical applicability.

Keywords: *Gold nanoparticles; Photochemotherapy; Radiotherapy; Aminolevulinic acid; K562 cells*

How to cite this article

Khosravi H, Saeedi S, Goodarzi A, Nikzad S, Amiri F, Farmani A. Evaluation of 5-aminolevulinic acid-functionalized gold nanoclusters for combined photodynamic and radiation therapy in K562 leukemia cells. Nanomed J. 2027; 14: 1-. doi: 10.22038/nmj.2026.96784.2443

Corrected Proof

INTRODUCTION

Various cancer treatment modalities exist, including surgery, radiotherapy, brachytherapy, chemotherapy, hormone therapy, and non-ionizing radiation techniques such as hyperthermia and photodynamic therapy (PDT). Among these, radiotherapy and PDT are two non-invasive approaches that have gained considerable attention. These therapies are often preferred over invasive procedures due to their ability to preserve tissue architecture, enhance patient safety, and minimize systemic toxicity (1).

Radiotherapy is an established component of cancer management and is used in more than half of patients with malignancies, either as a standalone treatment or alongside other therapeutic approaches (2). Its antitumor effects are largely mediated by ionizing radiation, which can cause DNA double-strand breaks, promote the formation of reactive oxygen species (ROS), and ultimately lead to cancer cell death. However, the effects of irradiation are not confined exclusively to malignant tissue, and normal cells located within or near the irradiated volume can also be adversely affected. Accordingly, an important objective of radiotherapy is to deliver an effective radiation dose to the tumor while minimizing exposure and injury to surrounding healthy tissues (3, 4).

PDT relies on the interaction between a photosensitizer (PS), molecular oxygen, and visible light to induce cytotoxicity. It offers advantages including precise targeting, minimal systemic side

* *Corresponding author(s):* Alireza Goodarzi, PhD, Department of Medical Laboratory Sciences, School of Paramedicine, Hamadan University of Medical Sciences, Hamadan, Iran. Phone: +98 9126176758, Email: *a_goodarzi58@yahoo.com*.

Note. This manuscript was submitted on June 23, 2026; approved on October 21, 2026.

© 2026. This work is openly licensed via CC BY 4.0. This is an Open Access article distributed under the terms of the Creative Commons Attribution License (https://creativecommons.org/licenses), which permits unrestricted use, distribution, and reproduction in any medium, provided the original work is properly cited.

effects, selective apoptosis induction, and improved patient quality of life (5, 6). However, PDT has inherent limitations, such as restricted light penetration depth, which limits its efficacy to superficial tumors (7, 8).

Gold nanoparticles (AuNPs) have attracted considerable attention as potential tools for addressing these limitations. Their tendency to accumulate within tumor tissue through the enhanced permeability and retention (EPR) effect, together with their high atomic number, makes them particularly relevant to radiation-based approaches. In addition, the surface plasmon resonance of AuNPs enables efficient conversion of incident light into heat, thereby providing potential benefits for both radiotherapy and light-based therapeutic strategies (9, 10). ALA serves as a precursor for the endogenous photosensitizer protoporphyrin IX (PpIX) and can consequently support photodynamic treatment following its conversion to PpIX, which preferentially accumulates in malignant cells (11). Nevertheless, the amount of PpIX generated from ALA may be insufficient for optimal PDT responses. Incorporating ALA into nanoparticle-based delivery systems may improve its cellular delivery and, consequently, enhance the effectiveness of PDT (12).

This work examined the therapeutic effects of PDT and radiotherapy, administered separately or in combination, using ALA-functionalized gold nanoparticles in K562 cells. We hypothesized that the sequence of irradiation (laser vs. X-ray) would critically influence therapeutic outcome, with laser pre-treatment potentially sensitizing cells via sublethal ROS generation and mitochondrial perturbation, thereby enhancing subsequent radiation-induced cytotoxicity.

MATERIALS AND METHODS

Ethical approval

The study received ethical clearance from Hamadan University of Medical Sciences under approval number IR.UMSHA.REC.1400.819. K562 cells were sourced from the Pasteur Institute of Iran for use in the experiments.

Cell culture

Peripheral blood mononuclear cells (MNCs) obtained from a healthy donor served as the normal control group for comparison with the K562 leukemia cells. Venous blood was subjected to Ficoll-Paque density-gradient separation followed by centrifugation at 200 × g for 30 min at 4°C. The buffy coat containing the MNC fraction was collected and subsequently washed with phosphate-buffered saline (PBS). Both K562 cells and isolated MNCs were cultured in RPMI-1640 medium containing 10% fetal bovine serum (FBS) and 1% penicillin–streptomycin. Cultures were maintained at 37°C in a humidified incubator with 5% CO_2.

Synthesis and characterization of 5-ALA-functionalized gold nanoclusters

Gold nanoclusters were prepared by combining 0.15 mL of glutathione solution was added together with 4.35 mL of ultrapure water, after which the mixture was stirred continuously at 70°C for 24 h. ALA functionalization of the glutathione-stabilized nanoclusters was then pursued through ester-bond formation involving the available functional groups of glutathione. The morphology and particle size were evaluated by transmission electron microscopy (Figure 1). More extensive physicochemical characterization, including FTIR spectroscopy, zeta-potential measurement, polydispersity index (PDI), and UV–Vis spectroscopy, was not performed in this pilot study and represents a limitation of the present work.

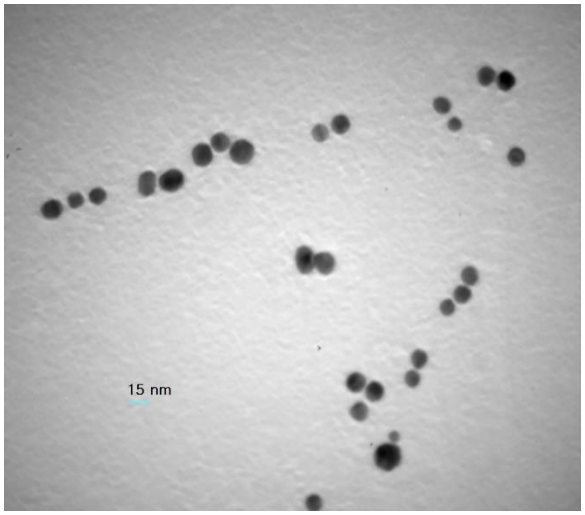


Fig. 1. A Transmission Electron Microscopy image of the synthesized GNPs

Corrected Proof

Determination of optimal nanoparticle concentration

Prior to treatment, the toxicity of the nanoparticles was assessed via MTT assay. Nanoparticles were synthesized using different gold solution concentrations (3, 5, 7, and 9 mM) and a fixed amino acid concentration (25 mM) to optimize the formulation.

Experimental design and treatment groups

To improve clarity, the experimental groups were systematically designed as follows (n=3 per group)

Group	Treatment Description
Control	Untreated cells
Group 1	RT alone (2 Gy)
Group 2	RT alone (4 Gy)
Group 3	5-ALA-AuNPs alone (optimal concentration)
Group 4	5-ALA-AuNPs + RT (2 Gy)
Group 5	5-ALA-AuNPs + RT (4 Gy)
Group 6	5-ALA-AuNPs + Laser alone
Group 7	5-ALA-AuNPs + Laser **before** RT (2 Gy)
Group 8	5-ALA-AuNPs + Laser **before** RT (4 Gy)
Group 9	5-ALA-AuNPs + Laser **after** RT (2 Gy)
Group 10	5-ALA-AuNPs + Laser **after** RT (4 Gy)

Treatment and Irradiation

Approximately 10,000 cells were seeded in 96-well plates and incubated for 24 hours. Cells were treated with 5-ALA-AuNPs at concentrations of 1.25, 0.625, and 0.3125 mg/mL. Laser irradiation (810 nm, 0.1 W) was applied for 60 seconds per well. The laser parameters were selected based on preliminary dose-response assays to achieve sub-lethal photodynamic priming. For RT, cells were exposed to 2 or 4 Gy using a 6 MeV linear accelerator. The sequence of irradiations followed the group designations above.

Assessment of cell viability

At 48 h after treatment, 0.5 mg/mL MTT solution was added to the wells, and the plates were incubated for an additional 4 h. The plates were subsequently centrifuged at 2000 rpm for 8 min, after which the supernatant was discarded. To solubilize the resulting formazan crystals, 100 µL of DMSO was added to each well. Absorbance was then measured at 570 nm, and cell viability was calculated as follows:

Viability (%) = [Absorbance (treated) / Absorbance (control)] × 100.

Statistical analysis

Results are expressed as mean ± SD. Depending on the distribution of the data, differences among groups were evaluated using either one-way ANOVA or the Kruskal–Wallis test, with Bonferroni adjustment applied for post-hoc comparisons. Statistical significance was defined as $p < 0.05$.

RESULTS

The mean viability values across all groups are reported in Tables 1–8. The Kruskal–Wallis test indicated significant differences among groups ($p < 0.001$).

Overall efficacy of combined treatments

Among the treatment conditions evaluated, Group 8 (Nano + Laser before + 4 Gy) produced the greatest reduction in cell viability, with a mean viability of 27.01%, indicating the strongest cytotoxic response. Conversely, cells receiving 2 Gy of radiotherapy alone showed the highest mean viability (63.84%), suggesting the least pronounced treatment effect among the groups (Table 1, Figure 2). Bonferroni-adjusted pairwise analysis demonstrated statistically significant differences in viability between most treatment groups, although several group pairs did not differ significantly from one another (Table 2).

Corrected Proof

Table 1. Mean, standard deviation, 95% confidence interval, minimum and maximum viability in treatment groups

Group	Mean	SD	95% CI		Minimum	Maximum
			Lower	Upper		
Control	100.0000	9.37751	88.3563	111.6437	89.33	108.68
Nano	60.7867	2.02525	58.2720	63.3014	58.92	63.69
Nano + Laser	53.0240	3.83177	48.2662	57.7818	50.20	58.13
2 Gy	63.8420	1.23405	62.3097	65.3743	62.50	65.41
4 Gy	50.3340	2.51686	47.2089	53.4591	46.06	52.66
Nano +2 Gy	50.4907	2.12039	47.8579	53.1235	47.40	53.26
Nano + 4 Gy	42.7253	2.00002	40.2420	45.2087	40.10	44.72
Nnano + laser before + 2 Gy	39.8547	1.24235	38.3121	41.3972	38.05	41.44
Nano + laser before + 4 Gy	27.0120	2.67599	23.6893	30.3347	23.48	30.15
Nano + 2 Gy + laser after	47.8167	1.25171	46.2625	49.3709	45.62	48.53
Nano + 4 Gy + laser after	34.3180	.88933	33.2137	35.4223	32.91	35.30

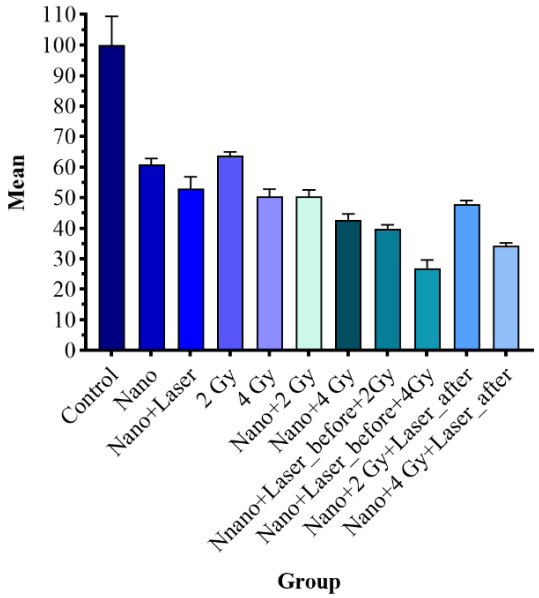


Fig. 2. Mean viability of the control and treatment groups

Table 2. Comparison of viability means between treatment groups

	Control	Nano	Nano + Laser	2 Gy	4 Gy	Nano + 2 Gy	Nano + 4 Gy	Nan o+ Laser before + 2Gy	Nano + Laser before + 4Gy	Nano + 2 Gy +Laser after	Nano + 4 Gy +Laser after
Control	<0.001	<0.001	<0.001	<0.001	<0.001	<0.001	<0.001	<0.001	<0.001	<0.001	
Nano		0.001	0.174	<0.001	<0.001	<0.001	<0.001	<0.001	<0.001	<0.001	
Nano + Laser			<0.001	0.230	0.258	<0.001	<0.001	<0.001	0.023	<0.001	
2 Gy				<0.001	<0.001	<0.001	<0.001	<0.001	<0.001	<0.001	
4 Gy					0.944	0.001	<0.001	<0.001	0.261	<0.001	
Nano + 2 Gy						0.001	<0.001	<0.001	0.232	<0.001	
Nano + 4 Gy							0.200	<0.001	0.026	<0.001	
Nano + Laser_before + 2 Gy								<0.001	0.001	0.016	
Nano + Laser_before+4Gy									<0.001	0.002	
Nano + 2 Gy + Laser after										<0.001	

Concentration-dependent effects

- ***Low concentration (0.3125 mg/mL):*** The highest viability (82.9%) was observed in the nanoparticle-only group, while the lowest (49.6%) was achieved with Nano + Laser before + 4 Gy (Table 3, Figure 3).
- ***Medium concentration (0.625 mg/mL):*** Nano alone showed 62.25% viability, whereas Nano + Laser before + 4 Gy reduced viability to 29.27% (Table 5, Figure 4).

Table 3. Mean, standard deviation, 95% confidence interval, minimum and maximum viability in the low-concentration treatment groups

Group	Mean	Std. Deviation	95% Confidence Interval		Minimum	Maximum
			Lower Bound	Upper Bound		
control	100.0000	9.37665	88.3573	111.6427	89.33	108.68
nano low	82.9159	4.07949	77.8506	87.9813	78.49	87.88
nano+laser low	74.3068	4.40936	68.8319	79.7817	67.87	78.49
nano+2 Gy low	69.5215	6.52917	61.4144	77.6285	60.15	78.49
nano+4 Gy low	58.2066	3.09505	54.3636	62.0496	54.34	61.49
nano+laserbefore+2Gy low	49.4410	3.26774	45.3835	53.4984	45.17	52.21
nano+laserbefore+4 Gy low	37.3882	6.17200	29.7246	45.0517	27.39	42.93
nano+2 Gy+laserafter low	67.0394	2.33138	64.1446	69.9341	64.29	69.21
nano+4 Gy+laserafter low	38.0590	1.05656	36.7471	39.3709	37.01	39.58

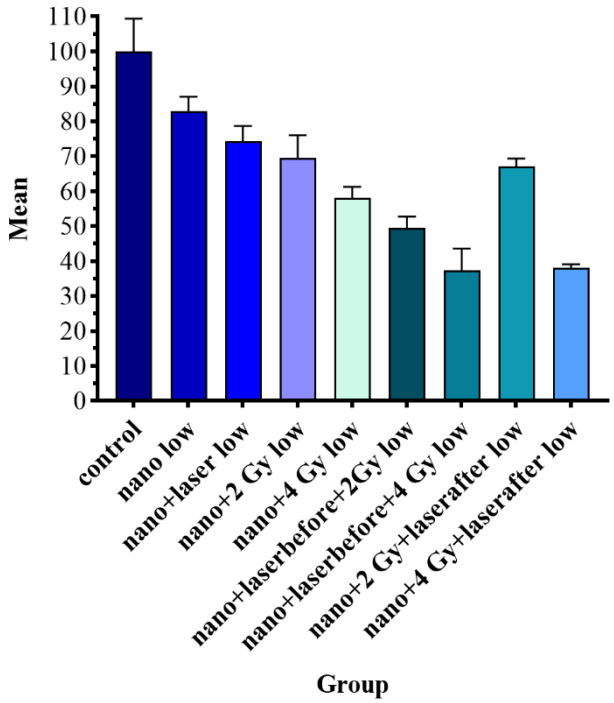


Fig. 3. The mean viability of the control and treatment groups at low concentrations.

Table 4. Comparison of viability means between treatment groups at low concentrations

	nano low	nano+laser low	nano+2 Gy low	nano+4 Gy low	nano+laserbefore+2 Gy low	nano+laserbefore+4 Gy low	nano+2 Gy+laserafter low	nano+4 Gy+laserafter low
control	<0.001	<0.001	<0.001	<0.001	<0.001	<0.001	<0.001	<0.001
nano low		0.007	<0.001	<0.001	<0.001	<0.001	<0.001	<0.001
nano+laser low			0.125	<0.001	<0.001	<0.001	0.022	<0.001
nano+2 Gy low				0.001	<0.001	<0.001	0.421	<0.001
nano+4 Gy low					0.007	<0.001	0.006	<0.001
nano+laserbefore+2Gy low						<0.001	<0.001	0.001
nano+laserbefore+4 Gy low							<0.001	0.827
nano+2 Gy+laserafter low								<0.001

Table 5. The mean, SD, 95% CI, minimum and maximum viability in the medium concentration treatment groups.

Group	Mean	Std. Deviation	95% Confidence Interval		Minimum	Maximum
			Lower Bound	Upper Bound		
control	100.0000	9.37665	88.3573	111.6427	89.33	108.68
nano medium	62.2540	3.08372	58.4251	66.0830	58.59	65.41
nano+laser medium	49.7470	5.18470	43.3094	56.1847	43.65	55.65
nano+2 Gy medium	50.6708	2.97330	46.9790	54.3627	45.73	53.78
nano+4 Gy medium	37.3435	2.64229	34.0626	40.6243	35.78	42.04
nano+laserbefore+2Gy medium	40.1834	2.27850	37.3542	43.0125	36.56	42.37
nano+laserbefore+4 Gy medium	29.2710	2.17147	26.5748	31.9673	27.28	32.65
nano+2 Gy+laserafter medium	47.6297	3.29024	43.5443	51.7151	44.05	52.77
nano+4 Gy+laserafter medium	35.7335	1.03263	34.4513	37.0156	34.55	36.90

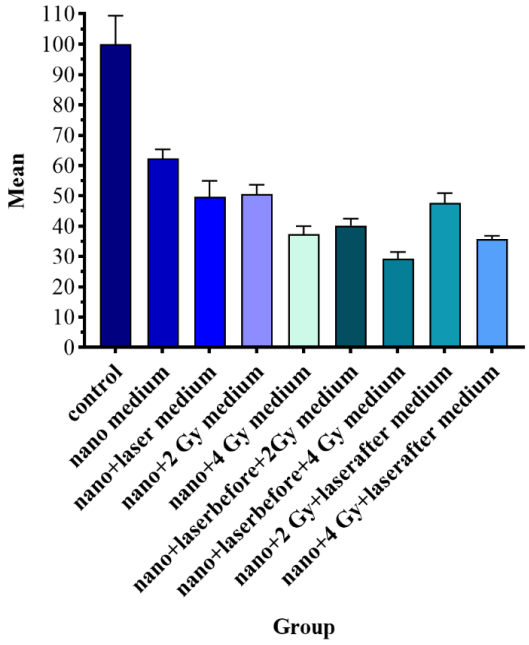


Fig. 4. The mean viability of the control and treatment groups at medium concentrations.

- ***High concentration (1.25 mg/mL):*** Treatment with Nano alone resulted in 37.18% viability. The Nano + Laser before + 4 Gy regimen produced the strongest reduction in viability, leaving only 14.37% viable cells (Table 7, Figure 5). All treatment groups at this concentration showed significantly lower viability than the control, with the laser-before-RT sequence demonstrating the greatest cytotoxic effect.

Table 6. Comparison of viability means between treatment groups with medium concentrations

	control	nano medium	nano+laser medium	nano+2 Gy medium	nano+4 Gy medium	nano+laserbefore+2 Gy medium	nano+laserbefore+4 Gy medium	nano+2 Gy+laserafter medium	nano+4 Gy+laserafter medium
control	<0.001	<0.001	<0.001	<0.001	<0.001	<0.001	<0.001	<0.001	
nano medium		<0.001	<0.001	<0.001	<0.001	<0.001	<0.001	<0.001	
nano+laser medium			0.724	<0.001	0.001	<0.001	0.419	<0.001	
nano+2 Gy medium				<0.001	<0.001	<0.001	0.248	<0.001	
nano+4 Gy medium					0.280	0.003	0.538	<0.001	
nano+laserbefore+2Gy medium						<0.001	0.007	0.094	
nano+laserbefore+4 Gy medium							<0.001	0.017	
nano+2 Gy+laserafter medium								<0.001	

Table 7. Mean, SD, 95% CI, minimum and maximum viability in the high-concentration treatment groups

Group	Mean	SD Deviation	95% CI		Minimum	Maximum
			Lower Bound	Upper Bound		
Control	100.0000	9.37665	88.3573	111.6427	89.33	108.68
Nano high	37.1869	3.29176	33.0997	41.2742	33.88	41.48
Nano + laser high	35.0179	4.20385	29.7981	40.2377	30.97	40.59
Nano + 2 Gy high	31.2835	1.57604	29.3266	33.2405	29.96	33.21
Nano + 4 Gy high	32.6252	3.62847	28.1199	37.1306	29.41	38.13
Nano + laser before +2 Gy high	29.9419	1.56210	28.0023	31.8815	27.73	31.75
Nano + laser before + 4 Gy high	14.3784	1.43531	12.5962	16.1605	12.75	16.32
Nano + 2 Gy + laser after high	28.7791	1.92132	26.3934	31.1647	26.39	31.08
Nano + 4 Gy + laser after high	29.1592	1.58000	27.1974	31.1210	26.61	30.30

Table 8. Comparison of viability means between treatment groups at high concentrations.

	Control	Nano high	Nano + laser high	Nano + 2 Gy high	Nano + 4 Gy high	Nano + laserbefore + 2 Gy high	Nano + laser before + 4 Gy high	Nano + 2 Gy +laser after high	Nano + 4 Gy + laser after high
Control		<0.001	<0.001	<0.001	<0.001	<0.001	<0.001	<0.001	<0.001
Nano high			0.395	0.025	0.079	0.007	<0.001	0.002	0.003
Nano + laser high				0.147	0.349	0.051	<0.001	0.018	0.026
Nano + 2 Gy high					0.598	0.598	<0.001	0.327	0.405
Nano + 4 Gy high						0.294	<0.001	0.136	0.177
Nano + laser before + 2 Gy high							<0.001	0.647	0.758
Nano + laser before + 4 Gy high								<0.001	<0.001
Nano + 2 Gy + laser after high									0.881

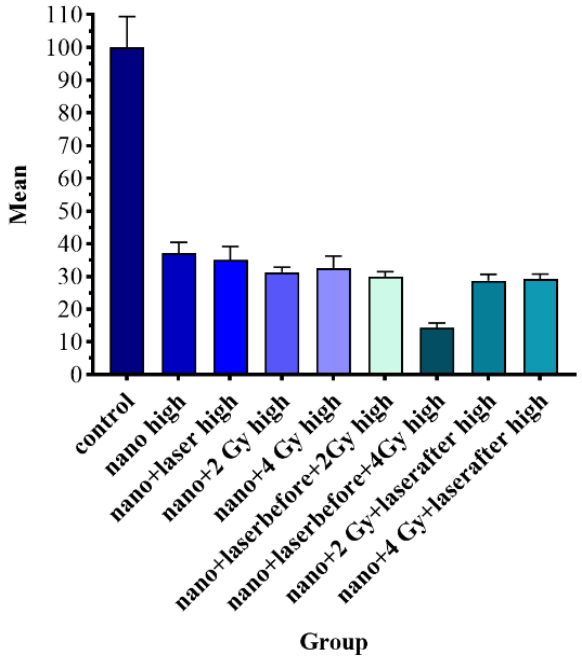


Fig. 5. The mean viability of the control and treatment groups at high concentrations.

DISCUSSION

Optimizing the combination of PDT and radiotherapy is critical for improving cancer outcomes. In this study, we evaluated the effects of 5-ALA-functionalized gold nanoparticles combined with RT and PDT on K562 cell viability. Our findings demonstrate that the "laser before radiotherapy" sequence, particularly at 4 Gy, yielded the most significant reduction in cell viability.

Mechanistic rationale for the Laser-Before-RT sequence

The superior efficacy of laser pre-treatment may be mechanistically rationalized as follows: upon laser irradiation, 5-ALA is converted to PpIX, which generates a burst of ROS (13). This early ROS wave can inflict sublethal oxidative damage to mitochondria and DNA, while simultaneously inhibiting DNA repair mechanisms (e.g., non-homologous end joining or homologous recombination) via oxidative modification of repair proteins (14). When ionizing radiation is subsequently applied, the cells are already "primed" with accumulated damage and impaired repair capacity, resulting in enhanced apoptosis or mitotic catastrophe. This hypothesis is supported by previous work showing that PDT can induce early apoptotic changes via the mitochondrial pathway, as demonstrated by Kuzelová et al. in K562 cells (15).

Role of gold nanoparticles

AuNPs contribute to radiosensitization through several mechanisms: physical dose enhancement due to high atomic number, ROS amplification, and induction of cell cycle arrest (16). The concentration-dependent effects observed in our study (highest cytotoxicity at 1.25 mg/mL) are consistent with this rationale. However, without direct cellular uptake studies, we cannot definitively confirm intracellular nanoparticle localization, which is a key limitation.

Comparison with literature

Our results align with studies by Xin et al., who showed that irradiation induces apoptosis via mitochondrial pathways and Bax/Bcl-xl modulation (17). Similarly, Xu et al. demonstrated that AuNP conjugates sensitized melanoma cells to 4 Gy radiation, partly via G2/M arrest (18). Mousavi et al. also reported enhanced cytotoxicity in glioblastoma cells exposed to 4 Gy with nanocomplexes (19). While these studies support our findings, they also underscore the need for mechanistic investigations—particularly regarding apoptosis, ROS quantification, and cell cycle analysis—which were absent in our current work.

Limitations

We acknowledge several critical limitations:

1. **Physicochemical characterization** (zeta potential, PDI, FTIR, drug loading) was incomplete.
2. **Mechanistic endpoints** (ROS, apoptosis, necrosis, cellular uptake) were not measured.
3. **No free 5-ALA control** was included, limiting our ability to attribute effects specifically to nanoparticle delivery.
4. The study is restricted to a single cell line (K562) and *in vitro* conditions.

Therefore, while our results are promising, they must be interpreted as preliminary proof-of-concept data requiring extensive follow-up.

CONCLUSIONS

This study demonstrates that 5-ALA-functionalized gold nanoparticles, when combined with laser and X-ray irradiation in a specific sequence (laser before radiotherapy), significantly enhance the killing of K562 leukemia cells. The sequence of treatment appears to be a critical variable influencing therapeutic efficacy, potentially through ROS-mediated priming and DNA repair inhibition. However, due to the lack of comprehensive nanoparticle characterization and mechanistic validation, these findings remain descriptive. Future work should include thorough physicochemical profiling, cellular uptake studies, ROS and apoptosis assays, and comparisons with free 5-ALA, alongside validation in additional cell lines and *in vivo* models, to establish the clinical translatability of this combined approach.

ACKNOWLEDGMENTS

The authors sincerely acknowledge the School of Dentistry at Hamadan University of Medical Sciences for providing access to the facilities necessary to perform the laser irradiation procedures in this study.

AUTHORS' CONTRIBUTIONS

H. Kh. and S. S. contributed to the conceptualization of the study. The methodology was developed by A. G. and S. N., while F. A. performed the formal analysis and A. G. conducted the investigation. Preparation of the original manuscript was undertaken by H. Kh., and all authors participated in reviewing and editing the manuscript. S. S. provided supervision and was responsible for funding acquisition, whereas project administration was handled by H. Kh.. All authors reviewed and approved the final version of the manuscript.

FUNDING

This research was funded by the Vice-chancellor for Research and Technology, Hamadan University of Medical Sciences (grant number 140104212703).

CONFLICT OF INTEREST

The authors declare no conflicts of interest.

ETHICS STATEMENT

Ethical approval for the study was granted by the Ethics Committee of Hamadan University of Medical Sciences (approval no. IR.UMSHA.REC.1400.819). The research was conducted in accordance with the principles of the Declaration of Helsinki. The K562 cell line was sourced from the Pasteur Institute of Iran (Tehran). Information regarding informed consent is provided through the institute's official website.

AI STATEMENT

No artificial intelligence tools were used for data generation, analysis, or scientific writing. AI was used solely for language polishing and grammar checking during manuscript preparation.

DATA AVAILABILITY

All study-related data underlying the reported findings are available in the published version of this article.

Corrected Proof

REFERENCES

1. Alsaab HO, Alghamdi MS, Alotaibi AS, Alzhrani R, Alwuthaynani F, Althobaiti YS, et al. Progress in clinical trials of photodynamic therapy for solid tumors and the role of nanomedicine. Cancers (Basel). 2020;12(10):2793.
2. Meyer P, Noblet V, Mazzara C, Lallement A. Survey on deep learning for radiotherapy. Comput Biol Med. 2018;98:126-146.
3. Begg AC, Stewart FA, Vens C. Strategies to improve radiotherapy with targeted drugs. Nat Rev Cancer. 2011;11(4):239-253.
4. Vissink A, Jansma J, Spijkervet F, Burlage F, Coppes R. Oral sequelae of head and neck radiotherapy. Crit Rev Oral Biol Med. 2003;14(3):199-212.
5. Brown SB, Brown EA, Walker I. The present and future role of photodynamic therapy in cancer treatment. Lancet Oncol. 2004;5(8):497-508.
6. Dolmans DEJGJ, Fukumura D, Jain RK. Photodynamic therapy for cancer. Nat Rev Cancer. 2003;3(5):380-387.
7. dos Santos AlF, De Almeida DRQ, Terra LF, Baptista McS, Labriola L. Photodynamic therapy in cancer treatment—an update review. J Cancer Metastasis Treat. 2019;5:25.
8. Mohammadi Z, Sazgarnia A, Rajabi O, Seilanian Toosi M. Comparative study of X-ray treatment and photodynamic therapy by using 5-aminolevulinic acid conjugated gold nanoparticles in a melanoma cell line. Artif Cells Nanomed Biotechnol. 2017;45(3):467-473.
9. Kim HS, Lee DY. Near-infrared-responsive cancer photothermal and photodynamic therapy using gold nanoparticles. Polymers (Basel). 2018;10(9):961.
10. Khaing Oo MK, Yang X, Du H, Wang H. 5-aminolevulinic acid-conjugated gold nanoparticles for photodynamic therapy of cancer. 2008. [Unpublished/Conference].
11. Shinoda Y, Kato D, Ando R, Endo H, Takahashi T, Tsuneoka Y, et al. Systematic review and meta-analysis of in vitro anti-human cancer experiments investigating the use of 5-aminolevulinic acid (5-ALA) for photodynamic therapy. Pharmaceuticals. 2021;14(3):229.
12. Pignatelli P, Umme S, D'Antonio DL, Piattelli A, Curia MC. Reactive oxygen species produced by 5-aminolevulinic acid photodynamic therapy in the treatment of cancer. Int J Mol Sci. 2023;24(10):8964.
13. Lopez RFV, Lange N, Guy R, Bentley MVLB. Photodynamic therapy of skin cancer: controlled drug delivery of 5-ALA and its esters. Adv Drug Deliv Rev. 2004;56(1):77-94.
14. Kuzelová K, Grebenová D, Pluskalová M, Marinov I, Hrkal Z. Early apoptotic features of K562 cell death induced by 5-aminolaevulinic acid-based photodynamic therapy. J Photochem Photobiol B. 2004;73(2):67-78.
15. Hirose K, Monzen S, Sato H, Sato M, Aoki M, Hatayama Y, et al. Megakaryocytic differentiation in human chronic myelogenous leukemia K562 cells induced by ionizing radiation in combination with phorbol 12-myristate 13-acetate. J Radiat Res. 2013;54(3):438-446.
16. Xin Y, Zhang HB, Tang TU, Liu GH, Wang JS, Jiang G, et al. Low-dose radiation-induced apoptosis in human leukemia K562 cells through mitochondrial pathways. Mol Med Rep. 2014;10:1569-157[illegible].
17. Xu W, Luo T, Li P, Zhou C, Cui [illegible], Pang B, et al. RGD-conjugated gold nanorods induce radiosensitization in melanoma cancer cells by downregulating αvβ3 expression. Int J Nanomedicine. 2012;7:915-924.
18. Mousavi M, Fesharshteh Koosha F, Neshastehriz A. Chemo-radiation therapy of U87-MG glioblastoma cells using SPIO@AuNP-Cisplatin-Alginate nanocomplex. Heliyon. 2023;9:e13847.
19. Adamczuk G.M, Humeniuk E, Adamczuk K, Madej-Czerwonka B, Dudka J. Disruption of mitochondrial function augments the radiosensitivity of prostate cancer cell lines. Ann Agric Environ Med. 2023;30(1):65-76.
20. Maddah A, Ziamajidi N, Khosravi H, Danesh H, Abbasalipourkabir R. Gold nanoparticles induce apoptosis in HCT-116 colon cancer cell line. Mol Biol Rep. 2022;49(8):7863-7871.
21. Khosravi H, Doosti-Irani A, Bouraghi H, Nikzad S. Investigation of gold nanoparticles effects in radiation therapy of cancer: a systematic review. J Adv Med Biomed Res. 2022;30(142):388-396.
22. Khosravi H, Ghazikhanlousani K, Rahimi A. Use of gold nanoparticles in MAGIC-f gels to 18 MeV photon enhancement. Nanomed J. 2019;6(1).
23. Khosravi H, Manoochehri H, Farmany A, Khoshghadam A, Rafieemehr H, Azmoonfar R. Bismuth selenide nanoparticles enhance radiation sensitivity in colon cancer cells in-vitro. Biochem Biophys Rep. 2024;38:101732.

Corrected Proof